Cosmogenic 3HE Measurements Provide Insight into Lithologic controls on Bedrock Channel Incision

Keen-Zebert, A.; Tooth, Stephen; Stuart, F. M.

Published in:
Journal of Geology

DOI:
10.1086/685506

Publication date:
2016

Citation for published version (APA):
Keen-Zebert, A., Tooth, S., & Stuart, F. M. (2016). Cosmogenic 3HE Measurements Provide Insight into Lithologic controls on Bedrock Channel Incision: Examples from the South African Interior. *Journal of Geology*, *124*(3). https://doi.org/10.1086/685506

Cosmogenic ^{3}He Measurements Provide Insight into Lithologic Controls on Bedrock Channel Incision: Examples from the South African Interior

A. Keen-Zebert,[1,2,]* *S. Tooth,*[2] *and F. M. Stuart*[3]

1. Division of Earth and Ecosystem Sciences, Desert Research Institute, Reno, Nevada 89512, USA; 2. Department of Geography and Earth Sciences, Aberystwyth University, Aberystwyth SY23 3DB, United Kingdom; 3. Isotope Geosciences Unit, Scottish Universities Environmental Research Centre, Rankine Avenue, Scottish Enterprise Technology Park, East Kilbride G75 0QF, United Kingdom

ABSTRACT

Resistant bedrock outcrops can exert control on river long-profile adjustment, upstream transmission of base level fall, and valley development, particularly in postorogenic settings. To examine how variation in lithologic resistance impacts landscape development in the postorogenic eastern South African interior, cosmogenic ^{3}He in pyroxene from Karoo dolerite was measured in samples from valleys of the Klip and Mooi Rivers and the Schoonspruit. The denudation rates measured from cosmogenic ^{3}He in the Klip and Mooi Rivers and the Schoonspruit are widely variable, with channel bed denudation rates ranging from 14 to 255 m/m.yr. and valley side and top denudation rates ranging from 11 to 50 m/m.yr. Various processes of channel bed erosion occurring at grain to block scales (abrasion, plucking, subaerial weathering) result in the widely ranging channel bed incision rates. In this setting, river incision rates are restricted by moderate unit stream powers (~20 to >50 W/m^2) and by limited sediment supply, resulting in a lack of abrasive tools. In many dolerite valleys, channel bed incision is commonly slow enough for local base levels to remain essentially stable for extended periods of time (>10 k.yr.). These results suggest that in the postorogenic eastern South African interior, resistant dolerite in channel long profiles can result in spatially variable rates of channel bed incision, with implications for the patterns and tempo of wider landscape dynamics.

Introduction

The influence of lithology on the nature and rates of fluvial processes is a key issue in landscape evolution studies owing to the importance of bedrock channel incision in setting the pace of landscape erosion (e.g., Howard et al. 1994; Whipple and Tucker 1999; Whipple et al. 2000; Wohl and Merritt 2001; Whipple 2004). The upstream propagation of base level fall in incising bedrock rivers is influenced by variable lithologic resistance to erosion, resulting in changing channel bed incision rates through space and time (Crickmay 1975; Twidale 1976, 1991, 1998; Bishop and Goldrick 2010; Jansen et al. 2010; Römer 2010; Adams 2012; Miller et al. 2013). This can result in spatially and temporally varying rates of sediment production and storage in catchments (Keen-Zebert et al. 2013) that may, at continental scales, influence rates of sediment delivery to deltaic and offshore environments.

Cosmogenic nuclides are widely used to constrain bedrock channel incision rates across multimillennial time scales, particularly where strath terraces and other geomorphic features provide clear markers of incision (e.g., Burbank et al. 1996, 2003; Hancock et al. 1998; Leland et al. 1998; Pratt et al. 2002; Bierman et al. 2004; Reusser et al. 2006; Seong et al. 2008). In the absence of tectonic or climatic drivers, the rates and processes of incision in bedrock channels are less well understood. In tectonically stable dryland settings, channel bed incision can be very slow (<10 m/m.yr.) and only slightly above background subaerial denudation rates over long time periods (e.g., Jansen 2006), which may result in little change in catchment

Manuscript received October 27, 2014; accepted December 21, 2015; electronically published April 25, 2016.

* Author for correspondence; e-mail: akz@dri.edu.

[The Journal of Geology, 2016, volume 124, p. 423–434] © 2016 by The University of Chicago.
All rights reserved. 0022-1376/2016/12403-0009$15.00. DOI: 10.1086/685506

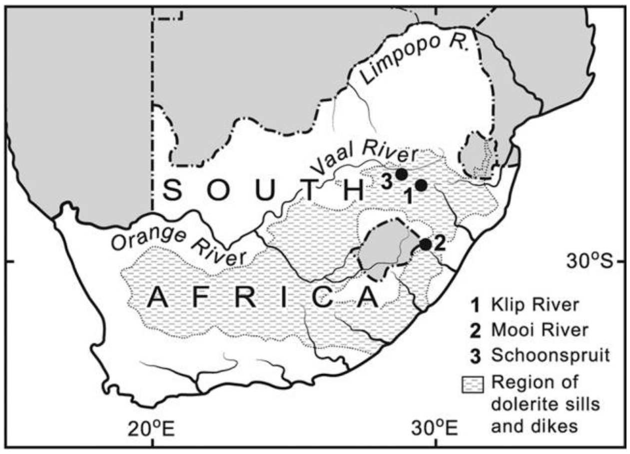

Figure 1. Map of South Africa showing the approximate limits of the main area of dolerite outcrop (simplified after Vorster 2003 and Decker et al. 2013) and the location of the three study reaches.

relief over time. However, at the landscape scale, spatial variation in erosional resistance can lead to the development of topography, even in the absence of uplift or climate change (e.g., Bishop and Brown 1992; Matmon et al. 2003; Jansen et al. 2010; Miller et al. 2013; Scharf et al. 2013; Bierman et al. 2014).

Although South Africa experienced tectonic activity following Gondwana breakup, it has been relatively stable throughout the Quaternary, albeit with some localized neotectonic activity (Andreoli et al. 1996; Bierman et al. 2014). Whereas the driver of post-Gondwana landscape development is contested, previous work suggests that one or more pre-Quaternary phases of epeirogenic uplift of the southern African subcontinent resulted in widespread river incision and backwearing or downwearing of slopes (Wellington 1955; King 1963; Partridge and Maud 1987; Gilchrist and Summerfield 1990, 1991; Gilchrist et al. 1994; Burke 1996; de Wit 1999, 2007; Moore 1999). Substantial thicknesses (1–2 km) of the Karoo Supergroup were eroded from across the interior (Hawthorne 1975; Partridge and Maud 1987; Gilchrist et al. 1994), and rivers have been superimposed onto varied lithologies with substantial variation in resistance (Tooth et al. 2002, 2004).

To contribute to understanding how resistant lithologies affect bedrock channel incision rates and landscape development, cosmogenic ^{3}He in pyroxene from Karoo Supergroup dolerite (diabase) was measured from three river valleys in the eastern South African interior. Unlike the more commonly used cosmogenic nuclides (^{10}Be and ^{26}Al), ^{3}He is routinely measured in mafic minerals (e.g., Kurz 1986; Cerling et al. 1994, 1999; Margerison et al. 2005; Evenstar et al. 2009) and can be used where felsic minerals are not abundant. The results are used to assess the implications of bedrock channel incision across lithologies with variable resistance in this tectonically stable dryland setting. Results are also compared with dolerite denudation rates measured elsewhere in South Africa (e.g., Kounov et al. 2007, 2009; Decker et al. 2011, 2013) and are discussed in the context of river incision and landscape evolution in postorogenic settings worldwide.

Regional Setting

Late Carboniferous to mid-Jurassic Karoo Supergroup lithologies crop out over approximately two-thirds of South Africa (Vorster 2003). Around the time of the Gondwana breakup, the predominantly marine and continental sedimentary successions of the Karoo Supergroup were extensively intruded by resistant dolerite sills and dikes (fig. 1) that formed feeders for widespread continental-scale flood basalts (Smith et al. 1993; Encarnación et al. 1996; Duncan et al. 1997; Jourdan et al. 2007; Svensen et al. 2007). The resistant dolerite sills and dikes now form topographic highs across much of the eastern, southern, and central interior (fig. 1) and are recognized as a key control in landscape development owing to their influence on regional drainage patterns, knickpoint retreat, and floodplain wetland distributions (e.g., Wellington 1955; King 1963; Tooth et al. 2002, 2004, 2013; Walcott

Table 1. Summary of Valley and Channel Characteristics

River system	Drainage area to the end of the study reach (km^2)	Slope	Unit stream power (W/m^2)	Channel width-to-depth ratio	Valley depth (m)
Klip River	1140[a]	>.003[a]	>45[a]	20	6–15
Schoonspruit	325[a]	>.002[a]	>20[a]	7	4–25
Mooi River	118[b]	>.003[b]	>50[b]	27	2–25

[a] Data reported by Tooth et al. 2004.
[b] Data reported by Grenfell et al. 2008.

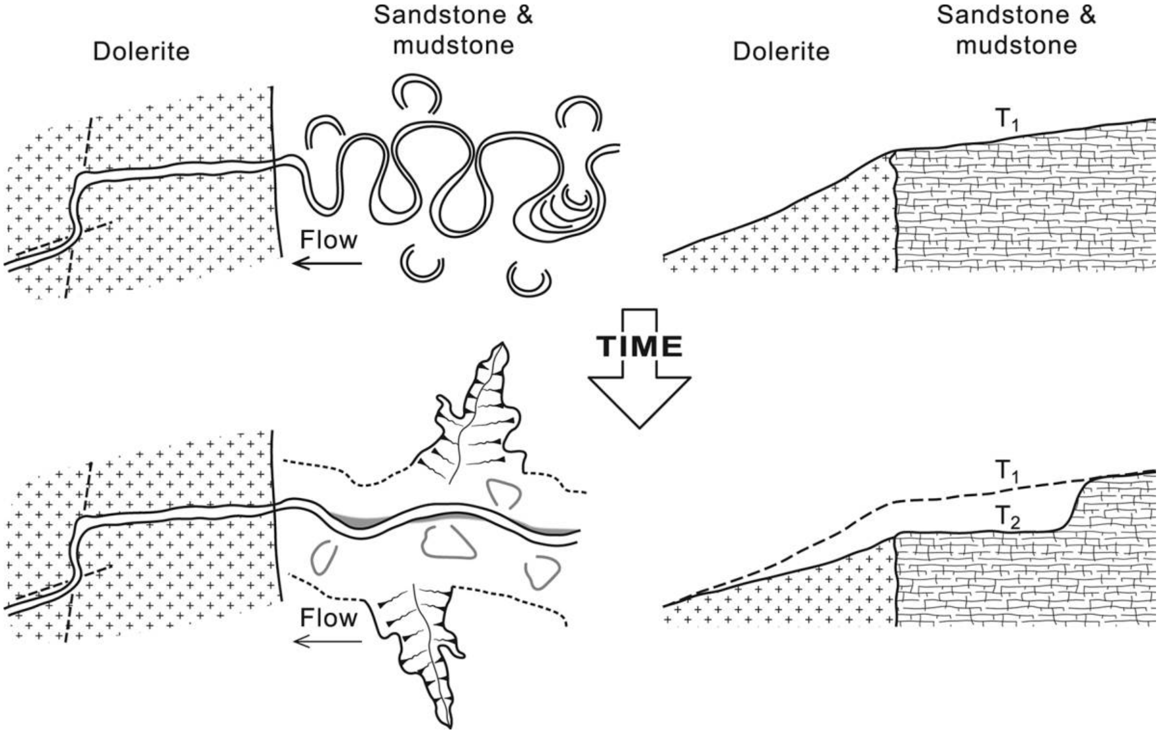

Figure 2. Schematic diagram illustrating the typical pattern of an unconfined, low-gradient reach on sedimentary rocks upstream of a confined, steeper reach developed in a dolerite sill or dike. A sinuous channel flanked by extensive floodplain wetlands changes downstream to a straighter channel with a narrow floodplain. Over time, bedrock channel incision in the confined reach may lead to partial incision (illustrated in the lower diagram) or complete incision through the sill or dike that promotes migration of a distinct knickpoint or a more diffuse knickzone into the upstream unconfined reach. As a result, the channel in the unconfined reach incises and straightens, and floodplain wetlands become decoupled from the channel, leading to desiccation and large gullies. Inset floodplains (gray shading) may form at a lower topographic level (after Tooth et al. 2004 and Keen-Zebert et al. 2013).

and Summerfield 2008; Keen-Zebert et al. 2013; fig. 2).

The Klip and Mooi Rivers and the Schoonspruit (fig. 1) are incised into the broad interior plateau of eastern South Africa and are subject to broadly similar climatic and hydrological conditions (table 1). The modern climate is subhumid with warm, wet summers and cool, dry winters. Mean annual rainfall in the catchment headwaters reaches a maximum of ~1200 mm and is exceeded by an annual potential evaporation of ~1400–2000 mm (Midgley et al. 1994; Schulze 1997). Limited river gauge data show that discharge regimes are strongly seasonal, with summer peak flows and winter low flows, and stream powers range from ~20 to >50 W/m^2 (table 1).

The study reaches are characterized by transitions from unconfined channels that migrate across wide floodplains underlain by relatively weak sandstones and mudstones to straighter, steeper, confined downstream reaches that are incised into more resistant dolerite (figs. 3, 4). In these confined reaches, the study rivers have different degrees of floodplain development, and bedrock valley depth varies from 2 to 25 m (table 1). Although the study rivers have different reach-scale geomorphology, the channel beds are generally characterized by dolerite bedrock that is orthogonally jointed, with joint spacing ranging from ~0.5 to 1 m in the horizontal plane and from ~0.2 to 0.5 m in the vertical plane. Locally plucked boulders separate pools in some reaches, but the mobile sediment load is negligible, with few cobbles and only minor granule-pebble gravel and sand bars present locally (fig. 5*A*). Following floods, stage falls rapidly, so large parts of the channel beds are dry for extended periods of time and are subaerially exposed.

Methods

Field Sampling Procedures. Samples were collected from the upstream ends of dolerite reaches that act as local base levels for upstream sandstone/

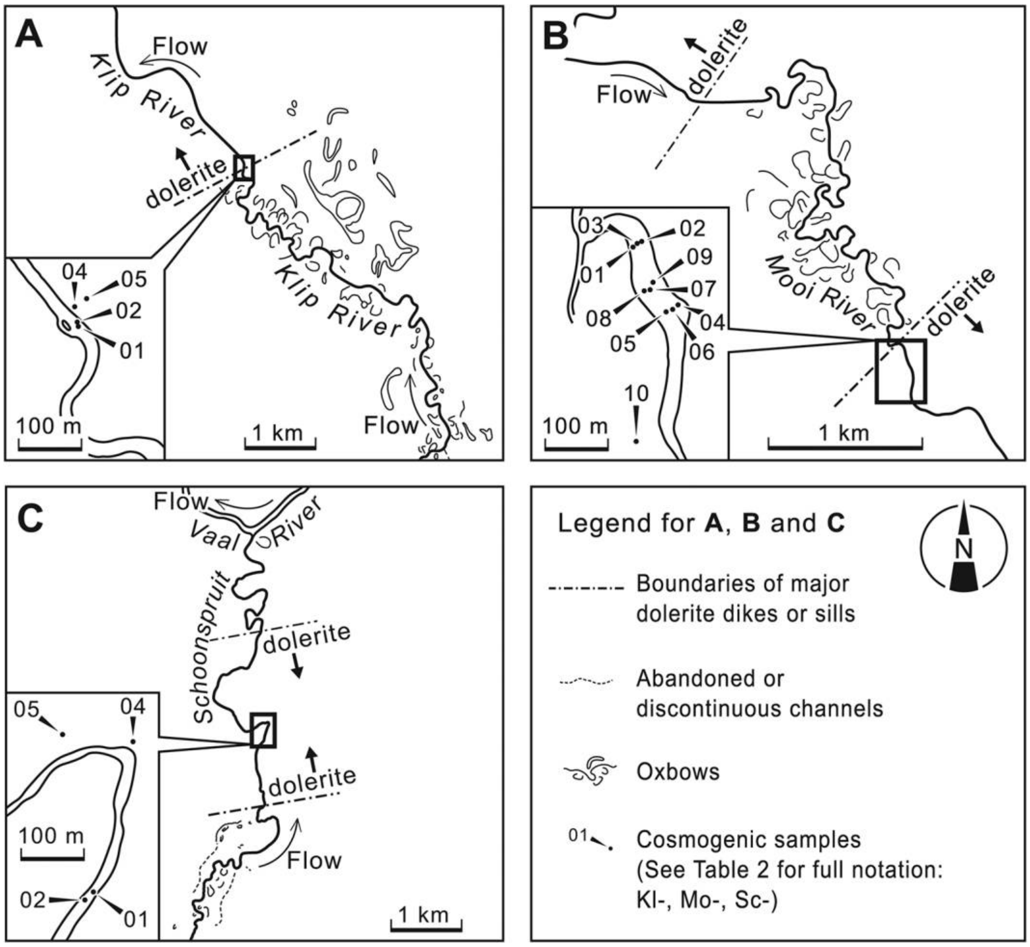

Figure 3. Geomorphological maps of the study reaches: *A*, Klip River; *B*, Mooi River; *C*, Schoonspruit. Insets show the locations of the samples collected for ^{3}He cosmogenic radionuclide analysis (see table 2 for sample site details). The rivers are all characterized by unconfined reaches with sinuous channels formed on erodible sandstones and mudstones that change downstream to confined reaches with straighter channels incised ~2–25 m into dolerite.

mudstone reaches that support floodplain wetlands (figs. 2, 3; Tooth et al. 2002, 2004; Keen-Zebert et al. 2013). On the Klip River and the Schoonspruit, two samples were collected from the channel beds (figs. 3–5; see fig. 5*A* and 5*C* for examples of sample collection sites). On the Mooi River, nine samples were collected from the channel bed from three valley cross sections along a prominent knickzone (figs. 3–5). Channel bed samples were collected from dolerite outcrop 0.3–2.0 m above low-water level. On the Klip and the Schoonspruit, one sample was collected from the valley sides (fig. 3*A*, 3*C*). A valley side sample could not be collected from the Mooi owing to lack of suitable exposure. In each study reach, one sample was also collected from a valley top location (figs. 3, 4; see fig. 5*B* and 5*D* for examples of sample collection sites). Shielded samples were collected at least 10 m below the surface from two quarries near the study reaches to quantify noncosmogenic ^{3}He, which can be produced via (n, α) reactions with ^{6}Li and magmatic ^{3}He trapped in melt inclusions (Niedermann 2002).

Samples were collected using a sledgehammer and chisel by exploiting natural joints and cracks. Sample locations and elevations were recorded by differential GPS survey (table 2). Topographic shielding was measured in the field, and all shielding factors were <0.993. Because samples were collected from elevated parts of the channel beds that do not retain water after floods (fig. 5*A*, 5*C*), in the subsequent analyses no correction for water shielding was made (Hancock et al. 1998; Reusser et al. 2006). Sediment accumulation in the channel bed is limited at the upstream ends of the dolerite reaches where the samples were collected (fig. 5*A*–5*C*), so no correction for shielding by bed sediment was made.

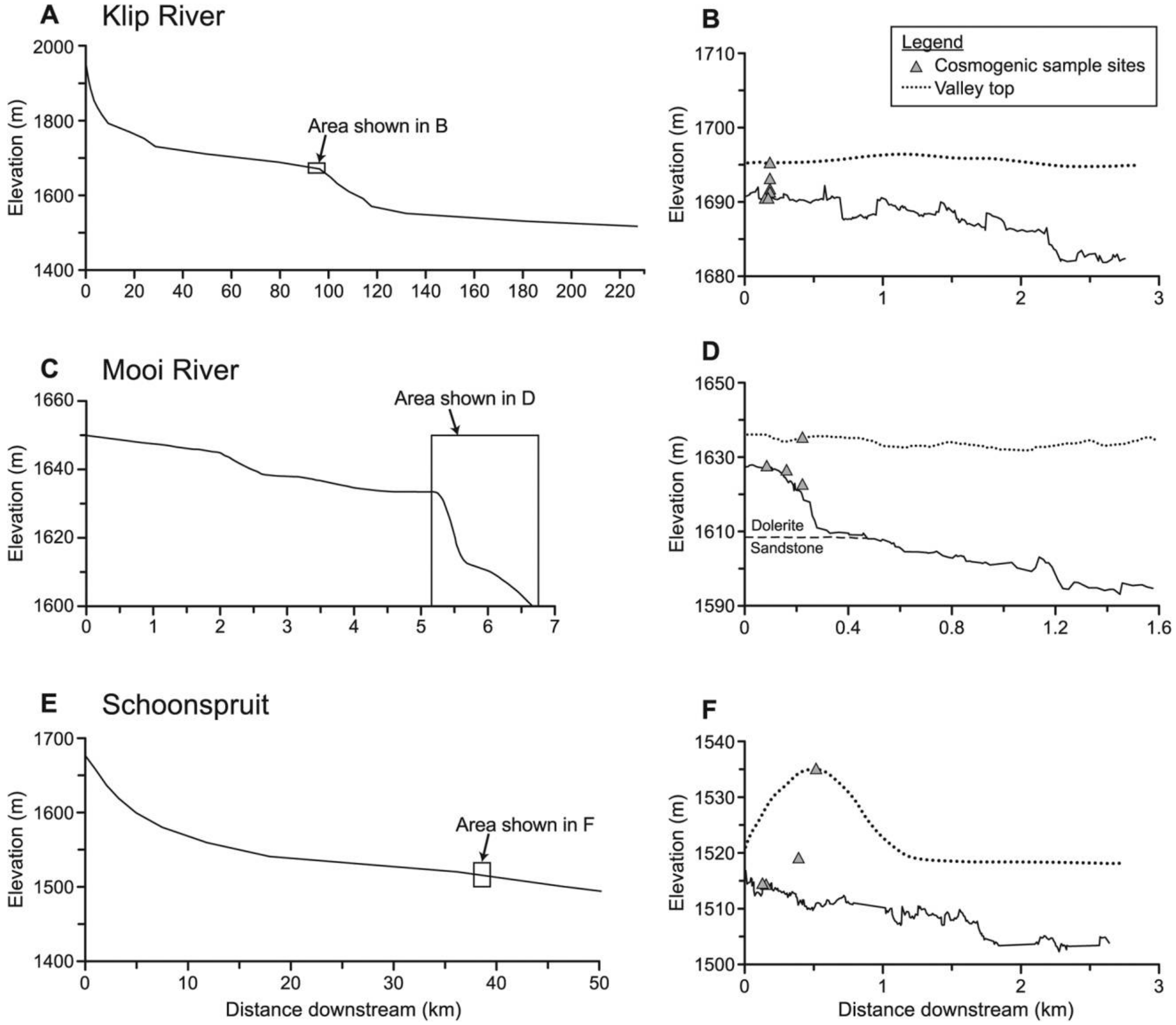

Figure 4. Long profiles for the study reaches: *A*, Klip River; *B*, Mooi River; *C*, Schoonspruit. Thalwegs and other landscape features were surveyed using differential GPS, and the locations of samples for cosmogenic ^{3}He measurements are indicated.

Laboratory Procedures and Analyses. The upper 3 cm of each sample was crushed and pyroxene was isolated from the 125–250-μm-sized fraction using a Frantz isodynamic magnetic separator. The pyroxene was then ultrasonically cleaned in 20% HNO_3 and distilled water, and pure pyroxene was picked under a binocular microscope. Altered grains and those with adhering plagioclase or iron oxide tarnish were removed, and the pure separate was cleaned in deionized water and then in analar acetone. Each sample was melted during a 10-min heating period using an 808-nm diode laser (Foeken et al. 2006). Reheating after the initial melt step yielded no significant ^{3}He. Gas cleanup procedures and mass spectrometric techniques for helium isotope ratio determination were similar to those reported by Williams et al. (2005) and Margerison et al. (2005). Blank levels were governed by the helium background in the mass spectrometer and average 5×10^3 and 5×10^8 atoms of ^{3}He and ^{4}He, respectively. The uncertainty ($\pm 30\%$) in the blank was incorporated into the calculated He concentrations. Blank corrections for ^{3}He and ^{4}He were minimal. The low ^{3}He of the Schoonspruit bedrock channel samples required a blank correction of 10%–20%. The reproducibility of standard He abundance determinations was 1% for ^{3}He and 0.5% for ^{4}He. The composition of the pyroxenes

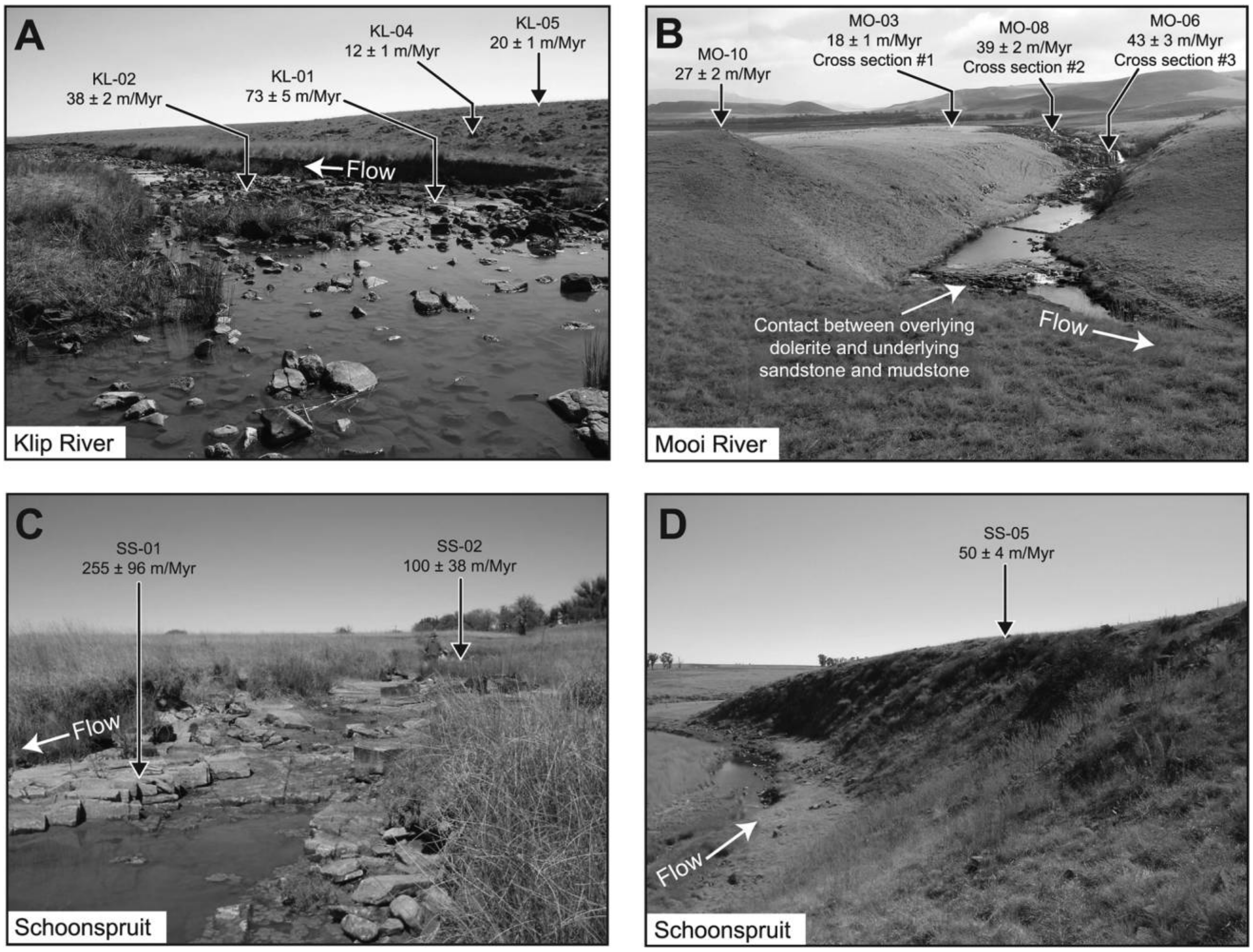

Figure 5. Photographs of the three study reaches illustrating typical characteristics of dolerite outcrop on channel beds, valley sides, and valley tops and examples of sample locations. In all three study reaches, the channel bed is largely devoid of sediment and is characterized by dolerite with horizontal and vertical joint spacing typically 0.2–1.0 m. Where present, channel bed sediment typically consists of <0.3-m-thick deposits of mud, sand, and granule to pebble gravel and/or locally plucked dolerite cobbles and boulders. The valley sides are low to steeply sloping, and the valley tops are of low relief. Valley sides and valley tops have very thin, discontinuous soil <0.5 m thick, and dolerite crops out extensively. *A*, Downstream view of the Klip River showing in situ fractured bedrock on the channel bed. *B*, Upstream view of the Mooi River showing the knickzone leading to a knickpoint, an incised valley downstream, and the low-relief valley top. The small knickpoint in the near foreground has formed where the channel has incised through the resistant dolerite and into the underlying weaker sandstone and mudstone (contact is indicated). *C*, Upstream view of the Schoonspruit showing plucked blocks on the channel bed and some large blocks remaining in situ. *D*, Downstream view of the Schoonspruit illustrating at least 25 m of incision into the dolerite sill. A color version of this figure is available online.

was determined using an electron microprobe at the University of Kentucky.

The concentration of cosmogenic ^{3}He in each exposed sample was calculated by subtracting the average of the concentration of ^{3}He in the shielded samples. In all but one case, cosmogenic ^{3}He greatly exceeds the concentration of inherited ^{3}He, demonstrating that exposure-generated He dominates the budget and can be used to quantify the rate of earth surface processes for the samples (table 2). Steady-state denudation rates (table 2) were calculated for a rock density of 3.05 g/cm^3 and an attenuation length of 150 g/cm (Gosse and Phillips 2001). Cosmogenic ^{3}He production rates in the pyroxene were calculated using the mean global olivine-based production rate (Goehring et al. 2010) scaled for the chemical composition of the pyroxenes using the elemental production rates of Masarik and Reedy (1995) and were scaled for latitude and altitude using the factors of Dunai

Table 2. Cosmogenic ^{3}He Concentrations and Denudation Rates of Dolerites from the Eastern Interior of South Africa

Description of sample location	Sample	Altitude (m)	Mass (g)	Lat (°S)	Long (°E)	^{4}He (10^{-7} ccSTP/g)	^{3}He/^{4}He (R/R_a)[a]	Cosmogenic ^{3}He (10^6 at/g)[b]	Production rate (^{3}He at/g/yr)	Exposure age (k.yr.)	Denudation rate (m/m.yr.)
Shielded:											
Vryheid Quarry	VH-01	NA	.0540	−27.73082	30.78553	5.0 ± .001	.04 ± .01	Average noncosmogenic ^{3}He: .72 ± .005	...	...	...
Vrede Quarry	VD-01	NA	.0620	−27.41072	29.16578	2.9 ± .001	.06 ± .01		...	...	...
Vrede Quarry	VD-02	NA	.0530	−27.41072	29.16578	3.6 ± .001	.06 ± .01		...	...	...
Klip River:											
Valley top	KL-05	1695	.0462	−27.45218	29.57773	5.5 ± .004	.35 ± .02	6.7 ± .36	257	26 ± 1	20 ± 1
Valley side	KL-04	1690	.0197	−27.45240	29.57773	7.6 ± .028	.41 ± .02	11.1 ± .59	256	43 ± 2	12 ± 1
Channel bed	KL-02	1688	.1114	−27.45241	29.57778	4.3 ± .008	.26 ± .01	3.6 ± .15	256	14 ± 1	38 ± 2
Channel bed	KL-01	1685	.1054	−27.45245	29.57780	1.7 ± .003	.41 ± .03	1.9 ± .13	255	7 ± 1	73 ± 5
Mooi River:											
Valley top	MO-10	1635	.0617	−29.38877	29.74024	4.8 ± .002	.31 ± .03	5.1 ± .41	261	19 ± 2	27 ± 2
Channel bed upstream cross section 1	MO-01	1627	.0501	−27.45205	29.57794	2.8 ± .003	.98 ± .04	9.9 ± .43	259	38 ± 2	14 ± 1
Channel bed upstream cross section 1	MO-02	1627	.0480	−29.38828	29.73999	3.2 ± .110	.78 ± .05	8.9 ± .47	260	34 ± 2	15 ± 1
Channel bed upstream cross section 1	MO-03	1627	.0570	−29.38821	29.74006	2.5 ± .006	.88 ± .05	7.7 ± .34	259	30 ± 1	18 ± 1
Channel bed middle cross section 2	MO-07	1626	.0908	−29.38928	29.74056	1.9 ± .170	.79 ± .11	5.0 ± .55	259	19 ± 2	27 ± 3
Channel bed middle cross section 2	MO-08	1625	.0502	−29.38889	29.74010	3.0 ± .002	.37 ± .02	3.6 ± .15	259	13 ± 1	39 ± 2
Channel bed middle cross section 2	MO-09	1626	.0497	−29.38886	29.74015	2.8 ± .003	.60 ± .05	5.7 ± .44	259	22 ± 2	24 ± 2
Channel bed downstream cross section 3	MO-05	1622	.0509	−29.38925	29.74066	2.8 ± .002	.50 ± .04	4.6 ± .35	259	17 ± 1	30 ± 2
Channel bed downstream cross section 3	MO-06	1620	.0502	−29.38932	29.74048	4.8 ± .003	.22 ± .02	3.2 ± .25	259	12 ± 1	43 ± 3
Channel bed downstream cross section 3	MO-04	1622	.0551	−29.38821	29.74006	2.6 ± .007	.81 ± .05	7.3 ± .42	259	28 ± 2	19 ± 1
Schoonspruit:											
Valley top	SS-05	1535	.0839	−27.08308	28.89199	2.6 ± .004	.31 ± .02	2.5 ± .18	226	10 ± 1	50 ± 4
Valley side	SS-04	1519	.0200	−27.08512	28.89117	8.7 ± .057	.27 ± .02	8.2 ± .64	226	36 ± 3	11 ± 1
Channel bed	SS-02	1514	.0293	−27.08503	28.89122	11.1 ± .005	.05 ± .02	1.4 ± .52	226	6 ± 2	100 ± 38
Channel bed	SS-01	1514	.0510	−29.39117	29.74005	5.1 ± .003	.06 ± .02	.6 ± .20	226	2 ± 1	255 ± 96

Note. NA = not applicable; STP = standard temperature and pressure.

[a] ^{3}He/^{4}He ratios (R) are normalized to the air ratio (R_a: 1.39×10^{-6}).

[b] Cosmogenic ^{3}He is calculated for the surface samples by subtracting the average ^{3}He measured in the shielded samples.

(2001) to enable direct comparison with previous measurements of ^{3}He in South African dolerite (Decker et al. 2011, 2013).

Results

The denudation rates measured from cosmogenic ^{3}He in the Klip and Mooi Rivers and the Schoonspruit are widely variable, with channel bed denudation rates ranging from 14 to 255 m/m.yr. and valley side and top denudation rates ranging from 11 to 50 m/m.yr. (table 2). Incision rates are fastest on the Schoonspruit and slower on the Klip and Mooi Rivers, but on the latter they tend to increase downstream through the knickzone from cross section 1 to cross section 3 (table 2). Results from discriminant and multivariate analyses to define groups within the data set yielded low confidence for multiple groups of denudation rates based on position (valley top, valley side, or channel bed). Because the proportion of correctly classified observations by the discriminant analysis was <0.5, we consider the measured denudation rates as a single population regardless of position in the landscape. The arithmetic mean is 45 m/m.yr. including outliers and is 28 m/m.yr. excluding outliers; the median is 27 m/m.yr., and the standard deviation is 56 m/m.yr. Two outliers (99 ± 38 and 255 ± 96 m/m.yr.) lie outside the 95% confidence interval, which ranges from 17 to 74 m/m.yr. Both of the outliers are for channel bed samples on the Schoonspruit (table 2).

Interpretation and Discussion

Various processes of channel bed erosion occurring at grain to block scales result in the wide range in channel bed denudation rates observed in the study reaches (table 2). Field observations indicate that channel bed incision occurs primarily through plucking of joint-bounded blocks (block plucking), which are ~0.05–0.5 m^3 (fig. 5*A*, 5*C*). Potholing also contributes to channel bed incision but appears to be widespread only on the Mooi River at the downstream end of the knickzone. Channel bed surfaces lack evidence of widespread polishing, fluting, or scalloping, suggesting either that abrasion is a minor contributor to channel bed erosion or that subaerial weathering and erosion between floods removes these features. Stage falls rapidly after floods, leaving large parts of the channel bed exposed to subaerial weathering processes. In the subhumid, seasonally dry climate, moisture is limited on the elevated parts of the channel bed where samples were collected, and although most channel bed samples had well-developed iron or manganese oxide coatings, weathering rinds were very thin (<1 mm). Adjacent to the channel beds, weathering and mass loss on valley sides and tops may also result from range fires that are set annually as a pasture management practice to initiate the early growth of grasses (Govender et al. 2006). Following a range fire downstream of the Klip River study reach in 2008, field observations of freshly exposed dolerite surfaces adjacent to blackened outer surfaces suggest that some spalling occurs during fires, similar to observations in other studies (Bierman and Gillespie 1991; Zimmerman et al. 1994). On channel beds, valley sides, and valley tops, granular disintegration, spalling, spheroidal exfoliation, and pitting are readily apparent along the edges and corners of higher joint-bounded blocks, particularly where neighboring blocks have been removed.

In summary, these field observations show that mass is shed from the dolerite at grain to 0.5-m-thick block scales, episodically exposing underlying rock with lower concentrations of cosmogenic nuclides, so that samples from adjacent and otherwise similar-looking outcrops may have significantly different cosmogenic nuclide concentrations. The lowest denudation rates on the channel beds (14–15 m/m.yr.) likely represent grain-scale processes on blocks that are still attached to the bedrock. The highest denudation rates (99 ± 38 and 255 ± 96 m/m.yr.) likely represent sites where an overlying block was very recently removed. Owing to the varied scales of mass loss from the dolerite and the intermittent nature of the processes contributing to incision in the study reaches, a representative channel incision rate is likely to lie somewhere between the highest and lowest values, similar to studies of denudation on granitic inselbergs (Bierman and Caffee 2002) and other bedrock exposures (Nishiizumi et al. 1993).

This study complements and extends previous cosmogenic-derived denudation rates that were measured on dolerite outcrop on high interfluve surfaces and interpreted as climatically determined background subaerial denudation rates (e.g., Kounov et al. 2007, 2009; Decker et al. 2011, 2013). For example, based on 22 samples collected from dolerite outcrop on escarpments, high pavements, and the tops of inselbergs across the arid southwestern to more humid eastern parts of southern South Africa, denudation rates are typically <3.5 m/m.yr., although a few outliers with rates up to ~9 m/m.yr. were interpreted as reflecting episodic mass loss from surfaces, such as by exfoliation (Decker et al. 2013). The results of this study show that denudation rates in the immediate vicinity of river valleys tend to be higher; in particular, the rates on channel beds in our study reaches reflect the influence of both fluvial processes during floods (e.g., plucking, abrasion) and subaerial weathering processes in the intervals between floods (e.g., granular disintegration, spalling). Defining such channel bed denudation rates is important because dolerite outcrop is widespread across South Africa (fig. 1), and the sills and dikes are important controls on landscape development, particularly through their influence on fluvial processes (fig. 2).

The results of this study also support and extend findings from other postorogenic dryland landscapes, particularly by exemplifying a common scenario whereby lithologies with variable resistance are exposed at the land surface during denudation. In the study reaches, fluvial processes have carved valleys into the dolerite sills and dikes, but like the situation in inland southeast Australia, where rivers are eroding resistant valley-filling basalt flows (Bishop and Goldrick 2010), incision rates are restricted by moderate stream powers and by limited sediment supply, which means a lack of abrasive tools. In many dolerite valleys, channel bed incision is slow enough for local base levels to remain essentially stable for extended periods of time. For example, in the study area optically stimulated luminescence ages suggest widespread preservation of floodplain sediment >30 ka in the upstream unconfined reach of the Klip River and abundant late Pleistocene/Holocene floodplain sediment in the unconfined reaches of the Mooi River and the Schoonspruit (Tooth et al. 2007, 2009; Keen-Zebert et al. 2013).

As posited in other studies (e.g., Crickmay 1975; Twidale 1976, 1991, 1998; Bishop and Goldrick 2010; Jansen et al. 2010; Römer 2010; Adams 2012), bedrock channels and hillslopes upstream of stable base levels or slowly retreating knickpoints become detached from base-level changes downstream, leading to spatially unequal geomorphological activity. In situations where resistant lithologies are widely distributed through a catchment (e.g., sills and dikes, multiple valley-filling basalt flows), catchments may become partitioned, with individual river reaches being adjusted to different local base levels. This partitioning of catchments by lithologic resistance can result in spatially variable rates of landscape evolution that can lead to net increases in catchment relief (e.g., Miller et al. 2013). Similar to investigations of river incision in some other postorogenic dryland landscapes, the results from the eastern South African interior demonstrate that resistant lithologies in channel long profiles can play a critical role in fluvial landscape dynamics.

ACKNOWLEDGMENTS

This material is based on work supported by the National Science Foundation under grant 0754345. Support was also provided by the Aberystwyth University Research Fund. J. Jansen has provided generous guidance throughout this study, from sampling strategy to manuscript review. Helium isotope analysis was conducted in the Scottish Universities Environmental Research Centre (SUERC) Noble Gas Laboratory with the assistance of L. DiNicola. We thank S. McCarthy and M. Kitching (University of the Witwatersrand) for facilitating fieldwork, Ezemvelo KZN Wildlife for permission to work within Kamberg Nature Reserve, and numerous landowners for permission to access their properties. We especially thank E. Muñoz-Salinas for many hours of pyroxene preparation. Figures were prepared by S. Baker at the Desert Research Institute and A. Smith at Aberystwyth University. Input from M. Rowberry and reviews by P. Bishop, P. Bierman, and R. Slingerland helped to guide the interpretation of the results and to significantly improve the manuscript.

REFERENCES CITED

Adams, K. M. 2012. Response of the Truckee River to lowering base level at Pyramid Lake, Nevada, based on historical air photos and LiDAR data. Geosphere 3:1–21.

Andreoli, M. A. G.; Doucoure, M.; Van Bever Donker, J.; Brandt, D.; and Anderson, N. J. B. 1996. Neotectonics of southern Africa: a review. Afr. Geosci. Rev. 3:1–16.

Bierman, P., and Gillespie, A. 1991. Range fires: a significant factor in exposure-age determination and geomorphic surface evolution. Geology 19:641–644.

Bierman, P.; Zen, E.; Pavich, M.; and Reusser, L. J. 2004. The incision history of a passive margin river, the Potomac near Great Falls. *In* Southworth, S., and Buron, W., eds. Geology of the National Capital Region: field trip guidebook for NE/SE Geological Society of America Meeting, Tysons Corner, Virginia, March 24–27, 2004. Reston, VA, USGS, p. 191–222.

Bierman, P. R., and Caffee, M. 2002. Cosmogenic exposure and erosion history of ancient Australian bedrock landforms. Geol. Soc. Am. Bull. 114:787–803.

Bierman, P. R.; Coppersmith, R.; Hanson, K.; Neveling, J.; Portenga, E. W.; and Rood, D. H. 2014. A cosmogenic view of erosion, relief generation, and the age of faulting in southern Africa. GSA Today 24:4–11.

Bishop, P., and Brown, R. 1992. Denudational isostatic rebound of intraplate highlands: the Lachlan River valley, Australia. Earth Surf. Process. Landf. 17:345–360.

Bishop, P., and Goldrick, G. 2010. Lithology and the evolution of bedrock rivers in post-orogenic settings: constraints from the high elevation passive continental margin of SE Australia. *In* Bishop, P., and Pillans, B., eds. Australian landscapes. Geol. Soc. Spec. Publ. 346:267–287.

Burbank, D. W.; Blythe, A. E.; Putkonen, J.; Pratt-Sitaula, B.; Gabet, E.; Oskin, M.; Barros, A.; and Ojha, T. P. 2003. Decoupling of erosion and precipitation in the Himalayas. Nature 426:652–655.

Burbank, D. W.; Leland, J.; Fielding, E.; Anderson, R. S.; Brozovic, N.; Ried, M. R.; and Duncan, C. 1996. Bedrock incision, rock uplift and threshold hillslopes in the northwestern Himalayas. Nature 379: 505–510.

Burke, K. 1996. The African plate. S. Afr. J. Geol. 99:341–409.

Cerling, T. E.; Poreda, R. J.; and Rathburn, S. L. 1994. Cosmogenic ^{3}He and ^{21}Ne age of the big lost river flood, Snake River plain, Idaho. Geology 22:227–230.

Cerling, T. E.; Webb, R. H.; Poreda, R. J.; Rigby, A. D.; and Melis, T. S. 1999. Cosmogenic ^{3}He ages and frequency of late Holocene debris flows from Prospect Canyon, Grand Canyon, USA. Geomorphology 27:93–111.

Crickmay, C. H. 1975. The work of the river. London, Macmillan.

Decker, J. E.; Niedermann, S.; and de Wit, M. J. 2011. Soil erosion rates in South Africa compared with cosmogenic ^{3}He-based rates of soil production. S. Afr. J. Geol. 114:475–488.

———. 2013. Climatically influenced denudation rates of the southern African plateau: clues to solving a geomorphic paradox. Geomorphology 190:48–60.

de Wit, M. 2007. The Kalahari epeirogeny and climate change: differentiating cause and effect from core to space. S. Afr. J. Geol. 110:367–392.

de Wit, M. C. J. 1999. Post-Gondwana drainage and the development of diamond placers in western South Africa. Econ. Geol. 94:721–740.

Dunai, T. J. 2001. Influence of secular variation of the geomagnetic field on production rates of in situ produces cosmogenic nuclides. Earth Planet. Sci. Lett. 193:1–16.

Duncan, R. A.; Hooper, P. R.; Rehacek, J.; Marsh, J. S.; and Duncan, A. R. 1997. The timing and duration of the Karoo igneous event, southern Gondwana. J. Geophys. Res. 102:18,127–18,138.

Encarnacion, J.; Fleming, T. H.; Eliot, D. H.; and Eales, H. V. 1996. Synchronous emplacement of Ferrar and Karoo dolerites and the early breakup of Gondwana. Geology 24:535–538.

Evenstar, L. A.; Hartley, A. J.; Stuart, F. M.; Mather, A. E.; Rice, C. M.; and Chong, C. 2009. Multi-phase development of the Atacama pediplain recorded by cosmogenic ^{3}He exposure ages: implications for Cenozoic climate change in western South America. Geology 37:27–30.

Foeken, J. P. T.; Stuart, F. M.; Dobson, K. J.; Persano, C.; and Vilbert, D. 2006. A diode laser system for heating minerals for (U-Th)/He chronometry. Geochem. Geophys. Geosyst. 7:Q04015.

Gilchrist, A. R.; Kooi, H.; and Beaumont, C. 1994. Post-Gondwana geomorphic evolution of southwestern Africa: implications for the controls on landscape development from observations and numerical experiments. J. Geophys. Res. 99:12,211–12,228.

Gilchrist, A. R., and Summerfield, M. A. 1990. Differential denudation and flexural isostasy in formation of rifted-margin upwarps. Nature 346:739–742.

———. 1991. Denudation, isostasy and landscape evolution. Earth Surf. Process. Landf. 16:555–562.

Goehring, B. M.; Kurz, M. D.; Balco, G.; Schaefer, J. M.; Licciardi, J.; and Lifton, N. 2010. A reevaluation of in situ cosmogenic ^{3}He production rates. Quat. Geochron. 5:410–418.

Gosse, J. C., and Phillips, F. M. 2001. Terrestrial in situ cosmogenic nuclides: theory and application. Quat. Sci. Rev. 20:1475–1560. doi:10.1016/S0277-3791(00)00171-2.

Govender, N.; Trollope, W. S. W.; and VanWilgen, B. W. 2006. The effect of fire season, fire frequency, rainfall and management on fire intensity in savanna vegetation in South Africa. J. Appl. Ecol. 46:748–758.

Grenfell, M. C.; Ellery, W.; and Grenfell, S. E. 2008. Tributary valley impoundment by trunk river floodplain development: a case study from the KwaZulu-Natal Drakensberg foothills, eastern South Africa. Earth Surf. Process. Landf. 33:2029–2044.

Hancock, G. S.; Anderson, R. S.; and Whipple, K. X. 1998. Beyond power: bedrock river incision process and form. *In* Tinkler, K. J., and Wohl, E. E., eds. Rivers over rock: fluvial processes in bedrock channels. Am. Geophys. Union Geophys. Monogr. 107: 35–59.

Hawthorne, J. B. 1975. Model of a kimberlite pipe. Phys. Chem. Earth 9:1–15.

Howard, A. D.; Dietrich, W. E.; and Seidl, M. A. 1994. Modeling fluvial erosion on regional to continental scales. J. Geophys. Res. 99:13,971–13,986.

Jansen, J. D. 2006. Flood magnitude–frequency and lithologic control on bedrock river incision in post-orogenic terrain. Geomorphology 82:39–57.

Jansen, J. D.; Codilean, A. T.; Bishop, P.; and Hoey, T. B. 2010. Scale dependence of lithological control on topography: bedrock channel geometry and catchment morphometry in western Scotland. J. Geol. 118:223–246.

Jourdan, F.; Feraud, G.; Bertrand, H.; Watkeys, M. K.; and Renne, R. R. 2007. Distinct brief events in the Karoo large igneous province clarified by new ^{40}Ar/^{39}Ar ages on the Lesotho basalts. Lithos 98:195–209.

Keen-Zebert, A.; Tooth, S.; Rodnight, H.; Duller, G. A. T.; Roberts, H.; and Grenfell, M. 2013. Late Quaternary floodplain reworking and the preservation of alluvial sedimentary archives in unconfined and confined river valleys in the eastern interior of South Africa. Geomorphology 185:54–66.

King, L. C. 1963. South African scenery: a textbook of geomorphology. 3rd ed. Edinburgh, Oliver & Boyd.

Kounov, A.; Niedermann, S.; de Wit, M. J.; Viola, G.; Andreoli, M.; and Erzinger, J. 2007. Present denudation rates at selected sections of the South African escarpment and the elevated continental interior based on cosmogenic ^{3}He and ^{21}Ne. S. Afr. J. Geol. 110:235–248.

Kounov, A.; Viola, G.; de Wit, M.; and Andreoli, M. A. G. 2009. Denudation along the Atlantic passive margin: new insights from apatite fission-track analysis on the western coast of South Africa. *In* Lisker, F.; Ventura, B.; and Glasmacher, U.A., eds. Thermochronological methods: from palaeotemperature constraints to landscape evolution models. Geol. Soc. Spec. Publ. 324:287–306.

Kurz, M. 1986. Cosmogenic helium in a terrestrial igneous rock. Nature 320:435–439.

Leland, J.; Reid, M. R.; Burbank, D. W.; Finkel, R.; and Caffee, M. 1998. Incision and differential bedrock uplift along the Indus River near Nanga Parbat, Pakistan Himalaya, from ^{10}Be and ^{26}Al exposure age dating of bedrock straths. Earth Planet. Sci. Lett. 154:93–107.

Margerison, H. R.; Phillips, W. M.; Stuart, F. M.; and Sugden, D. E. 2005. Cosmogenic ^{3}He concentrations in ancient flood deposits from the Coombs Hills, northern Dry Valleys, East Antarctica: interpreting exposure ages and erosion rates. Earth Planet. Sci. Lett. 230:163–175.

Masarik, J., and Reedy, R. C. 1995. Terrestrial cosmogenic-nuclide production systematics calculated from numerical simulations. Earth Planet. Sci. Lett. 136:381–395.

Matmon, A. S.; Bierman, P.; Larsen, J.; Southworth, S.; Pavich, M.; Finkel, R.; and Caffee, M. 2003. Erosion of an ancient mountain range, the Great Smoky Mountains, North Carolina and Tennessee. Am. J. Sci. 303:817–855.

Midgley, D. C.; Pitman, W. V.; and Middleton, B. J. 1994. Surface water resources of South Africa 1990. Vol. II. Pretoria, Water Research Commission.

Miller, S. R.; Sak, P. B.; Kirby, E.; and Bierman, P. R. 2013. Neogene rejuvenation of central Appalachian topography: evidence for differential rock uplift from stream profiles and erosion rates. Earth Planet. Sci. Lett. 369:1–12.

Moore, A. E. 1999. A reappraisal of epeirogenic flexure axes in southern Africa. S. Afr. J. Geol. 102: 363–377.

Niedermann, S. 2002. Cosmic-ray-produced noble gases in terrestrial rocks: dating tools for surface processes. Rev. Mineral. Geochem. 47:731–784.

Nishiizumi, K.; Kohl, C. P.; and Arnold, J. R. 1993. Role of in situ cosmogenic nuclides ^{10}Be and ^{26}Al in the study of diverse geomorphic processes. Earth Surf. Process. Landf. 18:407–425.

Partridge, T. C., and Maud, R. R. 1987. Geomorphic evolution of southern Africa since the Mesozoic. S. Afr. J. Geol. 90:179–208.

Pratt, B.; Burbank, D. W.; Heimsath, A. M.; and Ojha, T. 2002. Impulsive alleviation during early Holocene strengthened monsoons, central Nepal Himalaya. Geology 30:911–914.

Reusser, L.; Bierman, P.; Pavich, M.; Larsen, J.; and Finkel, R. 2006. An episode of rapid bedrock channel incision during the last glacial cycle, measured with ^{10}Be. Am. J. Sci. 306:69–102.

Römer, W. 2010. Multiple planation surfaces in basement regions: implications for the reconstruction of periods of denudation and uplift in southern Zimbabwe. Geomorphology 114:199–212.

Scharf, T. E.; Codilean, A. T.; de Wit, M.; Jansen, J. D.; and Kubik, P. W. 2013. Strong rocks sustain ancient postorogenic topography in southern Africa. Geology 41:331–334.

Schulze, R. E. 1997. South African atlas of agrohydrology and climatology. Report TT82/96. Pretoria, Water Research Commission.

Seong, Y. B.; Owen, L. A.; Bishop, M. P.; Bush, A.; Clendon, P.; Copland, L.; Finkel, R. C.; Ulrich, K.; and Shroder, J. F., Jr. 2008. Rates of fluvial bedrock incision within an actively uplifting orogens: Central Karakoram Mountains, northern Pakistan. Geomorphology 97:274–286.

Smith, R. M. H.; Eriksson, P. G.; and Botha, W. J. 1993. A review of the stratigraphy and sedimentary environments of the Karoo-aged basins of southern Africa. J. Afr. Earth Sci. 16:143–169.

Svensen, H.; Jamtveit, B.; Planke, S.; and Chevallier, L. 2007. Structure and evolution of hydrothermal vent complexes in the Karoo Basin, South Africa. J. Geol. Soc. 163:671–682.

Tooth, S.; Brandt, D.; Hancox, P. J.; and McCarthy, T. S. 2004. Geological controls on alluvial river behaviour: a comparative study of three rivers on the South African Highveld. J. Afr. Earth Sci. 38:79–97.

Tooth, S.; Hancox, P. J.; Brandt, D.; McCarthy, T. S.; Jacobs, Z.; and Woodborne, S. M. 2013. Controls on the genesis, sedimentary architecture, and preservation potential of dryland alluvial successions in stable continental interiors: insights from the incising Modder River, South Africa. J. Sediment. Res. 83:541–561.

Tooth, S.; McCarthy, T. S.; Brandt, D.; Hancox, P. J.; and Morris, R. 2002. Geological controls on the formation of alluvial meanders and floodplain wetlands: the example of the Klip River, eastern Free State, South Africa. Earth Surf. Process. Landf. 27: 797–815.

Tooth, S.; Rodnight, H.; Duller, G. A. T.; McCarthy, T. S.; Marren, P. M.; and Brandt, D. 2007. Chronology and controls of avulsion along a mixed bedrock-alluvial river. Geol. Soc. Am. Bull. 119:452–461.

Tooth, S.; Rodnight, H.; McCarthy, T. S.; Duller, G. A. T.; and Grundling, A. T. 2009. Late Quaternary dynamics of a South African floodplain wetland and the implications for assessing recent human impacts. Geomorphology 106:278–291.

Twidale, C. R. 1976. On the survival of palaeoforms. Am. J. Sci. 276:77–94.

———. 1991. A model of landscape evolution involving increased and increasing relief amplitude. Z. Geomorphol. 35:85–109.

———. 1998. Antiquity of landforms: an "extremely unlikely" concept vindicated. Aust. J. Earth Sci. 45:657–668.

Vorster, C. J. 2003. Simplified geology of South Africa, Lesotho, and Swaziland. Pretoria, South African Council for Geoscience.

Walcott, R. C., and Summerfield, M. A. 2008. Scale dependence of hypsometric integrals: an analysis of southeast African basins. Geomorphology 96:174–186.

Wellington, J. H. 1955. *In* Southern Africa: a geographical study. Vol. I. Physical geography. Cambridge, Cambridge University Press, 528 p.

Whipple, K. X. 2004. Bedrock rivers and the geomorphology of active origins. Annu. Rev. Earth Planet. Sci. 32:151–185.

Whipple, K. X.; Hancock, G. S.; and Anderson, R. S. 2000. River incision into bedrock: mechanics and relative efficacy of plucking, abrasion and cavitation. Geol. Soc. Am. Bull. 112:490–503.

Whipple, K. X., and Tucker, G. E. 1999. Dynamics of the stream-power river incision model: implications for height limits of mountain ranges, landscape response timescales, and research needs. J. Geophys. Res. 104:17,661–17,674.

Williams, A. J.; Stuart, F. M.; Day, S. J.; and Phillips, W. M. 2005. Using pyroxene microphenocrysts to determine cosmogenic ^{3}He concentrations in old volcanic rocks: an example of landscape development in central Gran Canaria. Quat. Sci. Rev. 24:211–222.

Wohl, E. E., and Merritt, D. M. 2001. Bedrock channel morphology. Geol. Soc. Am. Bull. 113:1205–1212.

Zimmerman, S. G.; Evenson, E. B.; Gosse, J. C.; and Erskine, C. P. 1994. Extensive boulder erosion resulting from a range fire on the Type-Pinedale Moraines, Fremont Lake, Wyoming. Quat. Res. 42: 255–265.